Phase structures of neutral dense quark matter and application to strange stars*

Shu-Sheng Xu(徐书生)[1†]

School of Science, Nanjing University of Posts and Telecommunications, Nanjing 210023, China

Abstract: In the contact interaction model, the quark propagator has only one solution, namely, the chiral symmetry breaking solution, at vanishing temperature and density in the case of physical quark mass. We generalize the condensate feedback onto the coupling strength from the 2 flavor case to the 2+1 flavor case, and find the Wigner solution appears in some regions, which enables us to tackle chiral phase transition as two-phase coexistences. At finite chemical potential, we analyze the chiral phase transition in the conditions of electric charge neutrality and β equilibrium. The four chemical potentials, μ_u, μ_d, μ_s and μ_e, are constrained by three conditions, so that one independent variable remains: we choose the average quark chemical potential as the free variable. All quark masses and number densities suffer discontinuities at the phase transition point. The strange quarks appear after the phase transition since the system needs more energy to produce a d-quark than an s-quark. Taking the EOS as an input, the TOV equations are solved numerically, and we show that the mass–radius relation is sensitive to the EOS. The maximum mass of strange quark stars is not susceptible to the parameter Λ_q we introduced.

Keywords: chiral phase transition, dense quark matter, quark stars

DOI: 10.1088/1674-1137/ac2f95

I. INTRODUCTION

It is well-known that hadrons with strangeness are unstable, they can decay into lighter hadrons made of non-strange quarks through the weak interaction. The hypothesis of stable strange nuclei was first proposed by A. Bodmer in Ref. [1]. Afterwards, E. Witten proposed stable dense quark matter containing strange quarks, based on the assumption that the Fermi momentum of the system exceeds the strange quark mass in the dense quark matter, therefore the dense quark matter favors the transformation of some non-strange quarks into strange quarks [2]. There are plenty of studies on strange quark stars from that time on [3-9]. Especially after the detection of gravitational waves from the merging of compact stars, people are interested in exploring the inner structure of compact stars [10-13].

The properties of dense QCD play a key role in the structure of compact stars, but lattice regularized QCD can not deal with such systems because of a technical difficulty, that is the "sign problem". Various models are inevitably used to study the phase structures of dense QCD systems, such as the quasi-particle model [14-20], quark-meson model [21-26], Nambu-Jona-Lasinio (NJL) model [48, 27-33], and some models of Dyson–Schwinger equations (DSEs) [34-46]. Based on these model studies, people believe that there are colorful phase structures in dense QCD matter. Most of these model studies find there is a critical endpoint (CEP) in the phase diagram. The chiral phase transition happens at low temperature and high density, while the low density and high-temperature region has a crossover. In terms of cold dense QCD, DSEs are confronted with the difficulty that the quark propagator has poles at high baryon chemical potential. The NJL model also has a drawback that there is only one solution in the non-chiral limit, and the pressure of the system is discontinuous at the chiral phase transition point, therefore the equation of state (EOS) is incomplete. In order to resolve this problem, the quark condensate feedback approach is proposed in the contact interaction model [47, 48]. In this approach, the coupling strength depends on the quark condensates, and the Wigner solu-

Received 24 September 2021; Accepted 14 October 2021; Published online 25 November 2021

* Supported in part by the National Natural Science Foundation of China (11905107), the National Natural Science Foundation of Jiangsu Province of China (BK20190721), Natural Science Foundation of the Jiangsu Higher Education Institutions of China (19KJB140016), Nanjing University of Posts and Telecommunications Science Foundation (NY129032), Innovation Program of Jiangsu Province

† E-mail: xuss@njupt.edu.cn

tion appears for some parameter choices.

In this work, we borrow this idea and extend it to 2+1 flavors to study dense QCD phase structure and strange quark stars. We give a basic introduction to the quark gap equation and the quark condensate feedback approach in the 2+1 flavor case in Sec. II, the solutions of the quark propagator are shown and related parameters are fixed by pion and kaon observables. In Sec. III, the dense QCD phase structures are studied in conditions of electric charge neutrality and β equilibrium. Using the EOS as an input, the mass–radius relation is given in Sec. IV. Finally, we summarize our studies in Sec. V.

II. QUARK PROPAGATORS IN VACUUM

The quark propagator plays a central role in many issues. It satisfies the Dyson–Schwinger equation,

$$S_f^{-1}(p) = S_{f0}^{-1}(p) + g^2 \int \frac{\mathrm{d}^4q}{(2\pi)^4} D_{\mu\nu}(p-q)\gamma_\mu t^a S_f(p)\Gamma_\nu^a(p,q), \tag{1}$$

where $S_{f0}(p)$ is the bare quark propagator with flavor f, $S_f(p)$ is the dressed quark propagator, t^a $(a=1,2,\cdots,8)$ are half of the Gell-Mann matrices, $\Gamma_\nu^a(p,q)$ is the amputated quark–gluon vertex, $D_{\mu\nu}(p-q)$ is the dressed gluon propagator. It is an exact equation, which is derived from a QCD generating functional. The quark propagator (two-point Green function) is related to the quark–gluon vertex (three-point Green function), and the three-point Green function is related to higher-point Green functions, so that there are infinite coupled integral equations. Thus, specific truncation for DSEs is necessary. We will use rainbow truncation, which is simple and preserves chiral symmetry, so that it is widely used in hadron physics as well as thermal and dense QCD:

$$\Gamma_\nu^a(p,q) \longrightarrow \gamma_\nu t^a. \tag{2}$$

The quark DSE is closed if the dressed gluon propagator is specified. We use the contact interaction model from Ref. [49], that is

$$g^2 D_{\mu\nu}(p-q) = \frac{1}{M_G^2}\delta_{\mu\nu}. \tag{3}$$

The quark DSE turns to be

$$S_f^{-1}(p) = S_{f0}^{-1}(p) + \frac{4}{3M_G^2}\int^\Lambda \frac{\mathrm{d}^4q}{(2\pi)^4}\gamma_\mu S_f(p)\gamma_\mu. \tag{4}$$

The integration in Eq. (4) with this model is divergent. The 3-dimension cut-off is performed in Ref. [50]. The inverse quark propagator has the general structure

$$S_f^{-1}(p) = \mathrm{i}\gamma\cdot pA_f(p^2) + B_f(p^2), \tag{5}$$

where $A_f(p^2)$ and $B_f(p^2)$ are two scalar functions. Substituting Eqs. (2), (3) and (5) into Eq. (1), one can obtain $A_f(p^2)=1$, $B_f(p^2)=M_f$. M_f is a constant mass, which satisfies

$$\begin{aligned} M_f &= m_f + \frac{4}{3M_G^2}\int^\Lambda \mathrm{Tr}_D[S_f(p)] \\ &= m_f + \frac{4}{3M_G^2}\int^\Lambda \frac{\mathrm{d}^4q}{(2\pi)^4}\frac{4M_f}{q^2+M_f^2} \\ &= m_f + \frac{2M_f}{3M_G^2\pi^2}\left[\Lambda\sqrt{\Lambda^2+M_f^2}\right. \\ &\quad \left. - M_f^2\ln\left(\frac{\Lambda}{M_f}+\sqrt{1+\frac{\Lambda^2}{M_f^2}}\right)\right]. \end{aligned} \tag{6}$$

There are four parameters in this model, namely $m_u=m_d$, m_s, M_G and Λ, which are fitted by pion mass m_π, pion decay constant f_π, kaon mass m_K, and light quark condensate $\langle\bar\psi\psi$ [51, 52]. The meson masses m_π, m_K are the solutions of their Bethe–Salpeter equations,

$$\Gamma_\pi(P) = -\frac{4}{3M_G^2}\int^\Lambda \frac{\mathrm{d}^4q}{(2\pi)^4}\gamma_\mu S_u(q_+)\Gamma_\pi(P)S_u(q_-)\gamma_\mu, \tag{7}$$

$$\Gamma_K(P) = -\frac{4}{3M_G^2}\int^\Lambda \frac{\mathrm{d}^4q}{(2\pi)^4}\gamma_\mu S_u(q_+)\Gamma_K(P)S_s(q_-)\gamma_\mu, \tag{8}$$

where $q_+=q+P/2$, $q_-=q-P/2$, and $P^2=-m_\pi^2$ for pion, $P^2=-m_K^2$ for kaon. The pion decay constant in 3 momentum cut-off is [50]

$$f_\pi^2 = N_c M_u^2 \int^\Lambda \frac{\mathrm{d}^3\vec{q}}{(2\pi)^3}\frac{1}{(\vec{q}^2+M^2)^{3/2}}. \tag{9}$$

The parameters and corresponding observables are listed in Table 1. To analyze the solution of the quark DSE, it is helpful to define a function

$$F(M_f) = M_f - m_f - \frac{2M_f}{3M_G^2\pi^2}C(M_f,\Lambda), \tag{10}$$

with

$$C(M_f,\Lambda) = \Lambda\sqrt{\Lambda^2+M_f^2} - M_f^2\ln\left(\frac{\Lambda}{M_f}+\sqrt{1+\frac{\Lambda^2}{M_f^2}}\right). \tag{11}$$

One can plot the function $F(M_f)$ for u- and s-quarks,

Table 1. Model parameters and observables in vacuum (all quantities in MeV).

m_u	m_s	M_G	Λ	M_u	M_s	m_π	m_K	f_π	$-\langle\bar{u}u\rangle^{\frac{1}{3}}$	$-\langle\bar{s}s\rangle^{\frac{1}{3}}$
4.3	110	189	799	314.6	547.5	139.3	498.2	93.3	292.2	327.6

as shown in Fig. 1. We can see that both functions have only one zero point, which implies there is only one solution in vacuum.

According to the gluon DSE, the inverse gluon propagator includes two parts, namely the pure Yang-Mills terms and the quark-loop term. The effective interaction between quarks, which is related to the dressed gluon propagator, should depend on the feedback of the quark-loop. Therefore, the effective interaction would be different for different solutions. Inspired by Ref. [47], we use the interaction

$$g^2 D_{\mu\nu}(k) = \delta_{\mu\nu}\frac{1}{M_{\rm eff}^2} = \delta_{\mu\nu}\left(\frac{1}{M_G'^2} - \sum_{f=u,d,s}\frac{1}{M_G'^2}\frac{\langle\bar{f}f\rangle}{\Lambda_f^3}\right), \quad (12)$$

where

$$\langle\bar{f}f\rangle = \frac{N_c M_f}{2\pi^2}C(M_f,\Lambda). \quad (13)$$

Although there are three energy scales Λ_f, we reduce the parameters, namely, use the same value $\Lambda_u = \Lambda_d = \Lambda_s = \Lambda_q$, in this work. The modified interaction introduces two new parameters, M_G' and Λ_q. As the first step, we fix $M_{\rm eff} = M_G$ in the Nambu solution and discuss the dependence of the parameters. This implies

$$M_G'^2 = M_G^2\left(1 - \sum_{f=u,d,s}\frac{\langle\bar{f}f\rangle}{\Lambda_q^3}\right). \quad (14)$$

The quark DSEs of 3 flavors are coupled to each other. We can define two functions,

$$\begin{aligned} F_u(M_u,M_s) &= M_u - m_u - \frac{2M_u}{3M_{\rm eff}^2\pi^2}C(M_u,\Lambda), \\ F_s(M_u,M_s) &= M_s - m_s - \frac{2M_s}{3M_{\rm eff}^2\pi^2}C(M_s,\Lambda). \end{aligned} \quad (15)$$

with $\frac{1}{M_{\rm eff}^2}$ as presented in Eq. (12). The solution is located at conditions $F_u(M_u,M_s)=0$ and $F_s(M_u,M_s)=0$. We plot these in Fig. 2. The green curved surface is $F_u(M_u,M_s)$ and the red is $F_s(M_u,M_s)$. We can see that there is only one solution if $\Lambda_q > 0.381$ GeV. When Λ_q decreases to 0.381 GeV, the second solution begins to appear. The third solution arises if $\Lambda_q < 0.381$ GeV, but Λ_q should be restricted between 0.30 GeV and 0.381 GeV if we require that the largest mass of the solution is the same as the original Nambu solution's mass. To this point, the model parameters are fixed except Λ_q. We use $\Lambda_q = 0.38$ GeV to study the properties of neutral dense

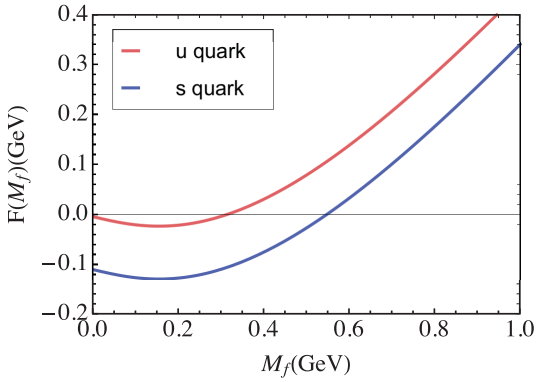

Fig. 1. (color online) The function $F(M_f)$ for u and s quarks.

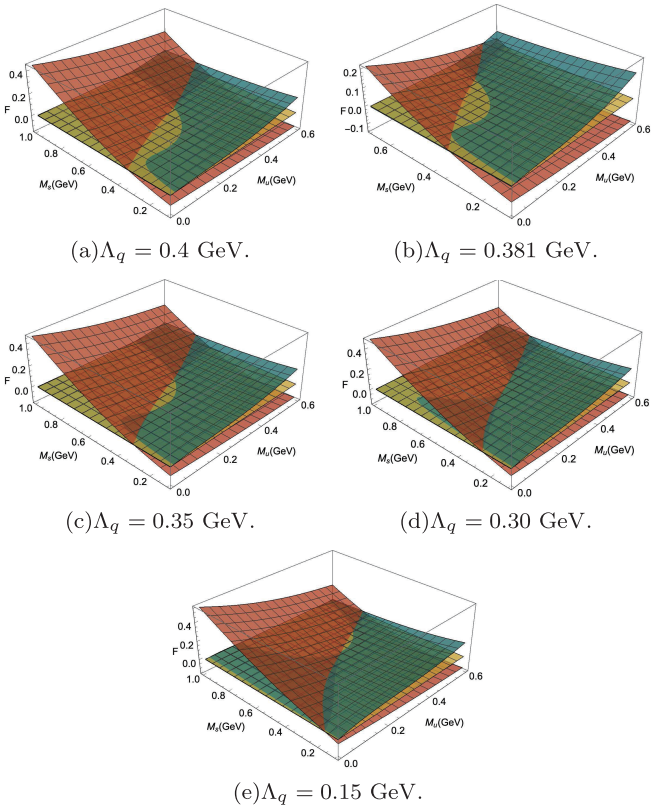

Fig. 2. (color online) F_u and F_s as functions of M_u and M_s. The green curved surface is F_u, the red is F_s, and the yellow is $F=0$. The intersections of three surfaces are the solutions of the quark DSEs.

quark matter in the next section. Afterwards, we will discuss the EOS and mass–radius relation dependence on Λ_q.

III. THE CHIRAL PHASE STRUCTURE IN NEUTRAL DENSE QUARK MATTER

We now turn our attention to the QCD system at finite chemical potential. The general structure of the inverse quark propagator is [1]

$$S_f^{-1}(p,\mu_f) = \mathrm{i}\gamma\cdot pA_f(p,\mu_f) + B_f(p,\mu_f) - \gamma_4 C_f(p,\mu_f). \quad (16)$$

Inserting Eq. (16) into Eq. (4), one can easily find that $A_f(p,\mu_f)=1$, $B_f(p,\mu_f)=M_f$, and $C_f(p,\mu_f)=\mu_f^*$ are constant quantities, where M_f and μ_f^* can be regarded as effective mass and chemical potential respectively. They satisfy

$$\begin{aligned} M_f &= m_f + \frac{4}{3M_{\rm eff}^2}\int^{\Lambda}\frac{\mathrm{d}^4q}{(2\pi)^4}\frac{4M_f}{q^2+M_f^2-\mu_f^{*2}+2i\mu_f^*q_4} \\ &= m_f + \frac{4}{3M_{\rm eff}^2}\int^{\Lambda}\frac{\mathrm{d}^3\vec{q}}{(2\pi)^4}\int_{-\infty}^{\infty}\mathrm{d}q_4\frac{4M_f}{q_4^2+2i\mu_f^*q_4+E_{qMf}^2-\mu_f^{*2}}, \end{aligned} \quad (17)$$

$$\begin{aligned} \mu_f^* &= \mu_f - \frac{4}{3M_{\rm eff}^2}\int^{\Lambda}\frac{\mathrm{d}^4q}{(2\pi)^4}\frac{2(iq_4-\mu_f^*)}{q_4^2+E_{qMf}^2-\mu_f^{*2}+2i\mu_f^*q_4} \\ &= \mu_f - \frac{8}{3M_{\rm eff}^2}\int^{\Lambda}\frac{\mathrm{d}^3\vec{q}}{(2\pi)^4}\int_{-\infty}^{\infty}\mathrm{d}q_4\frac{iq_4-\mu_f^*}{q_4^2+2i\mu_f^*q_4+E_{qMf}^2-\mu_f^{*2}}, \end{aligned} \quad (18)$$

with

$$E_{qMf} = \sqrt{\vec{q}^2+M_f^2}. \quad (19)$$

After some algebraic derivations, one finally obtains

$$M_f = m_f + \frac{2M_f}{3\pi^2M_{\rm eff}^2}\mathcal{D}(\mu_f^*,M_f), \quad (20)$$

$$\mu_f^* = \mu_f - \frac{2}{3\pi^2M_{\rm eff}^2}\left(\mu_f^{*2}-M_f^2\right)^{3/2}\theta(\mu_f^*-M_f), \quad (21)$$

$$\frac{1}{M_{\rm eff}^2} = \frac{1}{M_G'^2} + \sum_{f=u,d,s}\frac{1}{M_G'^2\Lambda_q^3}\frac{N_cM_f}{2\pi^2}\mathcal{D}(\mu_f^*,M_f), \quad (22)$$

with

$$\begin{aligned} \mathcal{D}(\mu_f^*,M_f) = &\left[\Lambda\sqrt{\Lambda^2+M_f^2} - M_f^2\ln\left(\frac{\Lambda}{M_f}+\sqrt{1+\frac{\Lambda^2}{M_f^2}}\right)\right] \\ &-\theta(\mu_f^*-M_f)\left[\mu_f^*\sqrt{\mu_f^{*2}-M_f^2}\right. \\ &\left.-M_f^2\ln\left(\frac{\sqrt{\mu_f^{*2}-M_f^2}}{M_f}+\frac{\mu_f^*}{M_f}\right)\right]. \end{aligned} \quad (23)$$

There is no difficulty in principle to solve the coupled Eqs. (20), (21) and (22) iteratively. Each quantity, such as effective mass and quark number densities, is a function of three different chemical potentials. In this work, we will focus on the phase structures in conditions of electric charge neutrality and β equilibrium. The β equilibrium requires

$$\mu_d = \mu_u + \mu_e, \quad (24)$$

$$\mu_s = \mu_d. \quad (25)$$

The condition of electric charge neutrality is

$$\frac{2}{3}n_u - \frac{1}{3}n_d - \frac{1}{3}n_s - n_e = 0, \quad (26)$$

where n_u, n_d, n_s and n_e are particle number densities for u-, d-, s-quarks and electron. We define the mean quark chemical potential by

$$\mu_q = \frac{\mu_un_u+\mu_dn_d+\mu_sn_s}{n_u+n_d+n_s}. \quad (27)$$

The four independent chemical potentials are constrained by three conditions, meaning there is only one independent chemical potential, so we are free to choose μ_q as independent. Effective masses of quarks varying with μ_q are displayed in Fig. 3. We can see from Fig. 3 that the Nambu solutions stay constant at $\mu_q < 315$ MeV, and disappear thereafter, while the Wigner solution exists on the whole region of quark chemical potential. In principle, the physical solution has a maximum pressure, and the bag constant, which is the pressure difference between Nambu and Wigner solutions in vacuum, is often introduced as a parameter in the NJL-like models. We assume the chiral phase transition happens at the location where the Nambu solution disappears, that is $\mu_q^c = 315$ MeV.

The dependencies of the quark number densities with μ_q are displayed in Fig. 4. The densities of u- and d-quark for the Nambu solution appear at 314.6 MeV and are very small compared to the densities of the Wigner solution. The densities suffer a discontinuity since nature

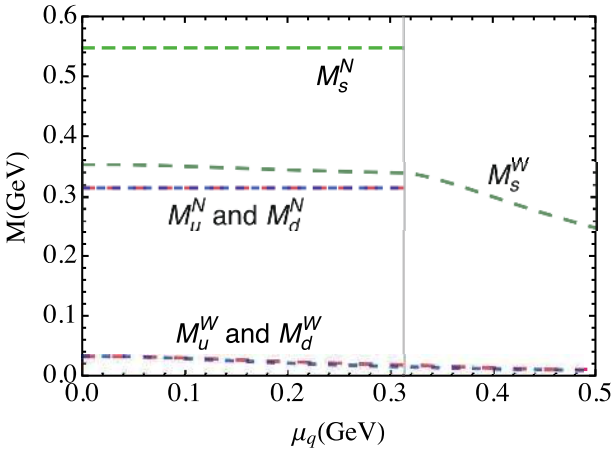

Fig. 3. (color online) Effective masses of quarks for both Nambu and Wigner solutions. The superscript 'N' means Nambu solution, 'W' means Wigner solution.

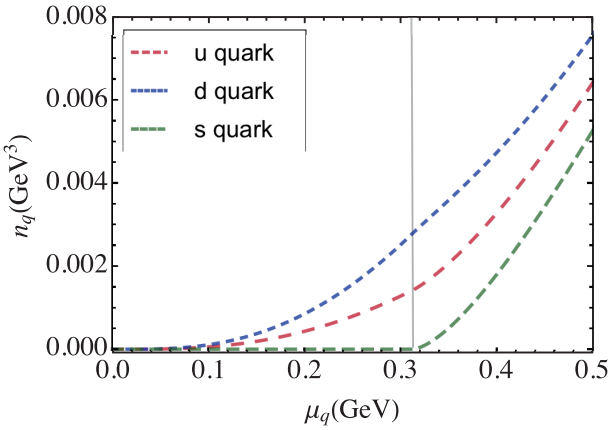

Fig. 4. (color online) Quark number densities as functions of μ_q.

chooses the Wigner solution at $\mu_q > \mu_q^c$. We can see that the s-quark appears very early because the quark condensates are smaller in the Wigner phase, which in turn affects the effective interaction strength. Nature also chooses the Wigner solution for the s quark, as its effective mass $M_s^W(\mu_q = 315\text{MeV}) = 339$ MeV is lower than its effective chemical potential $\mu_s^*(\mu_q = 315\text{MeV}) = 367$ MeV.

Based on our calculations, the densities of up and down quarks are very small, and the strange quark does not exist in the Nambu phase. After the chiral phase transition, nature favors the Wigner solution, all quarks have lower effective masses, and densities suffer discontinuities. The strange quark appears simultaneously. The transfer of chemical potentials is illustrated in Fig. 5.

IV. APPLICATION TO STRANGE QUARK STARS

The EOS of cold and dense quark matter plays a significant role in studying the structure of compact stars. We plot the EOS in Fig. 9, which is based on the phase

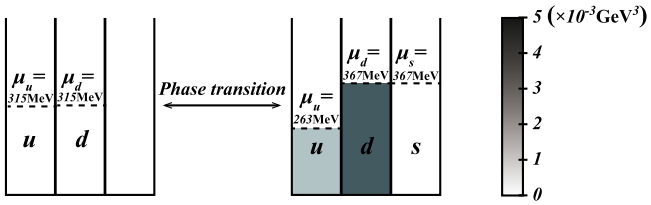

Fig. 5. (color online) Schematic illustration of the change of chemical potentials and quark number densities in the chiral phase transition. Quark number densities are represented by darkness.

properties of dense quark matter in conditions of electric charge neutrality and β equilibrium. The pressure is calculated by [53]

$$P(\mu_q) = \int_0^{\mu_q} \Big(n_u(\mu_q')\mathrm{d}\mu_u(\mu_q') + n_d(\mu_q')\mathrm{d}\mu_d(\mu_q') + n_s(\mu_q')\mathrm{d}\mu_s(\mu_q') + n_e(\mu_q')\mathrm{d}\mu_e(\mu_q')\Big). \tag{28}$$

This is related to the energy density:

$$\varepsilon(\mu_q) = -P(\mu_q) + \sum_i \mu_i(\mu_q) n_i(\mu_q). \tag{29}$$

The pressure, energy density and sound velocity $v_s = \sqrt{\dfrac{\partial P}{\partial \varepsilon}}$ as functions of μ_q are shown in Fig. 6, Fig. 7 and Fig. 8. The main range of sound velocity for strange quark matter is $0.52 < v_s/c < 0.62$, which meets the requirement of relativity.

In Fig. 9, we can see that the EOS tend to coincident in the large pressure region, while they have little difference at low pressure. This implies that the EOS is not too parameter-dependent in this model.

The relation between mass and radius of compact stars is governed by Tolman-Oppenheimer-Volkoff (TOV) equation,

$$\frac{\mathrm{d}P(r)}{\mathrm{d}r} = -\frac{G(\varepsilon+P)(M+4\pi r^3 P)}{r(r-2GM)}, \tag{30}$$

$$\frac{\mathrm{d}M(r)}{\mathrm{d}r} = 4\pi r^2 \varepsilon, \tag{31}$$

where natural units are used, $\hbar = 1 = c$. Taking the EOS as input into Eqs. (30) and (31), one can solve the TOV equation numerically. The mass–radius relation is illustrated in Fig. 10. We can see that the curves are apparently separate from each other, which indicates that the mass–radius relations are very sensitive to the EOS. The maximum mass of the strange quark star is (2.39, 2.45, 2.51)$M_\odot$ for $\Lambda_q =$ (0.30, 0.35, 0.38) GeV respectively.

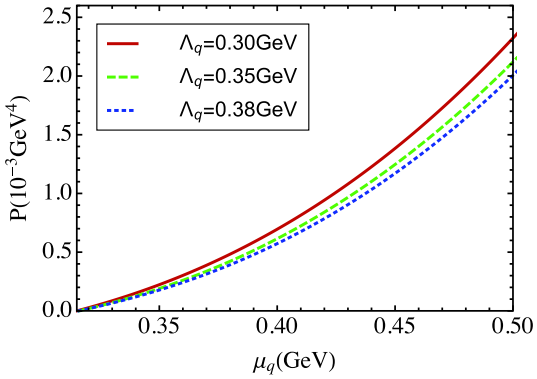

Fig. 6. (color online) Pressure as function of μ_q with three parameters.

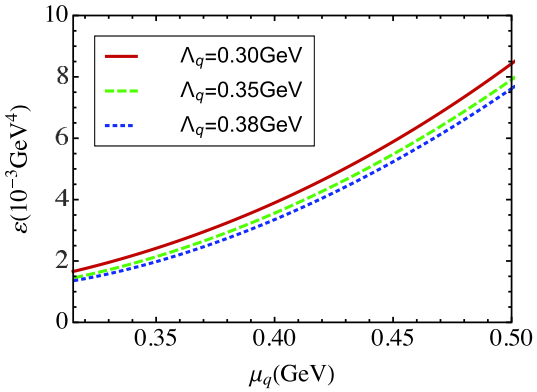

Fig. 7. (color online) Energy density as function of μ_q with three parameters.

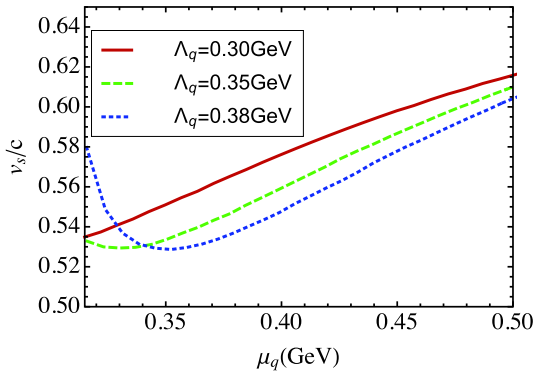

Fig. 8. (color online) Sound velocity as function of μ_q with three parameters.

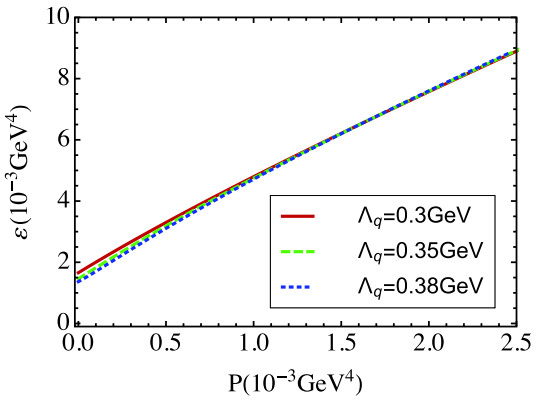

Fig. 9. (color online) EOS for three different parameters.

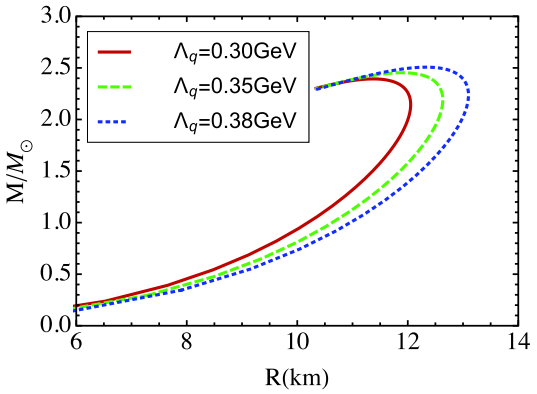

Fig. 10. (color online) Mass-radius relation for strange quark stars.

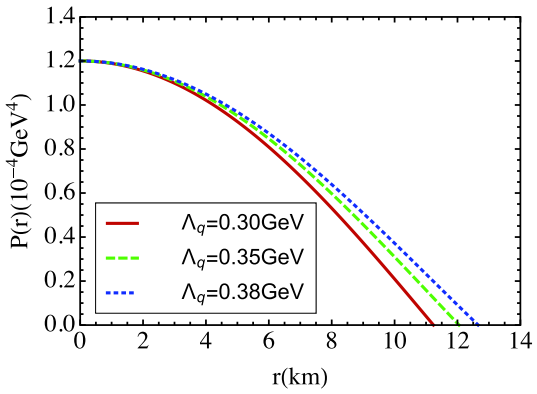

Fig. 11. (color online) Radius dependence of pressure at $P(0) = 1.2\times10^{-4}$ GeV^4 for $\Lambda_q = (0.3, 0.35, 0.38)$ GeV.

We find that the maximum mass is not sensitive to the parameter Λ_q. In order to show the details of the radius dependence of pressure, $P(r)$ is plotted in Fig. 11. We take the central pressure $P(0) = 1.2\times10^{-4}$ GeV^4 as an example for three cases of parameters $\Lambda_q = (0.3, 0.35, 0.38)$ GeV.

V. SUMMARY AND DISCUSSION

We have generalized the two-flavor contact interaction model to the three-flavor case, with the model parameters fitted by pion and kaon observables. Analyzing the solution of the quark DSE, there is only one solution, Nambu solution or chiral symmetry breaking solution, in vacuum. Based on the ideas from Refs. [47, 48], we introduce a feedback term from quark condensates to the coupling strength. The Wigner solution appears at some region of Λ_q. We mainly discuss $\Lambda_q \in (0.3, 0.381)$ GeV, since the Nambu and Wigner solutions coexist and the

largest mass equals the original Nambu value.

After fixing the model parameters, we studied the chiral phase transition in the conditions of electric charge neutrality and β equilibrium. During the phase transition, all quark masses and number densities suffer discontinuities. The strange quark appears since nature favors the lower effective mass, and $\mu_s^* > M_s$. At the phase transition point, the two phases coexist. The u-quark has smaller chemical potential in the chiral symmetry partially restored phase, while d-quark has larger value of chemical potential. Therefore, the system would need more energy to produce a d-quark than a s-quark if the density of the s-quark is very small.

The EOS of dense quark matter with neutrality is shown for three different Λ_q. They are almost coincident in the large pressure region, and have little difference at low pressure. Taking EOS as inputs to the TOV equations, the mass–radius relation for strange quark stars are drawn, which are very sensitive to the EOS. The maximum mass of strange quark stars is not susceptible to the parameter Λ_q. Its value reaches $2.39M_\odot$ or even $2.51M_\odot$.

The strange quark has two effects on the EOS; one is the quark condensate feedback, another is the nonzero strange quark number density diminishing the energy density. Comparing with the two flavor case of the NJL model, the maximum mass of strange star is larger than that of neutron star [54]. The strange stars are investigated with various models, such as the quasi-particle model and the NJL model [55, 56]. The mass–radius relation is qualitatively consistent with these studies. In Ref. [57], the authors analyze strange stars using observational data of the GW170817 and GW190425 binary mergers. The inferred mass–radius relation is close to our curve with $\Lambda_q = 0.38$ GeV.

References

[1] A. R. Bodmer, Phys. Rev. D **4**, 1601 (1971)
[2] E. Witten, Phys. Rev. D **30**, 272 (1984)
[3] M. G. Alford, K. Rajagopal, S. Reddy *et al.*, Phys. Rev. D **73**, 114016 (2006)
[4] P. Jaikumar, S. Reddy, and A. W. Steiner, Phys. Rev. Lett. **96**, 041101 (2006)
[5] S. Chakrabarty, Phys. Rev. D **43**, 627 (1991)
[6] R. Tikekar and K. Jotania, Pramana **68**, 397 (2007)
[7] F. Rahaman, K. Chakraborty, P. K. F. Kuhfittig *et al.*, Eur. Phys. J. C **74**, 3126 (2014), arXiv:1406.4118[gr-qc]
[8] M. Kalam, A. A. Usmani, F. Rahaman *et al.*, Int. J. Theor. Phys. **52**, 3319 (2013), arXiv:1205.6795[gr-qc]
[9] E. Zhou, A. Tsokaros, K. b. o. Uryū *et al.*, Phys. Rev. D **100**, 043015 (2019)
[10] I. Bombaci, A. Drago, D. Logoteta *et al.*, Phys. Rev. Lett. **126**, 162702 (2021)
[11] G. Wiktorowicz, A. Drago, G. Pagliara *et al.*, Astrophys. J. **846**, 163 (2017), arXiv:1707.01586 [astro-ph.HE]
[12] W. Husain and A. W. Thomas, AIP Conf. Proc. **2319**, 080001 (2021), arXiv:2010.06750[hep-ph]
[13] A. Kuerban, J.-J. Geng, and Y.-F. Huang, in AIP Conference Proceedings, Vol. 2127 (AIP Publishing LLC, 2019), p. 020027
[14] P. K. Srivastava, S. K. Tiwari, and C. P. Singh, Phys. Rev. D **82**, 014023 (2010)
[15] S. Plumari, W. M. Alberico, V. Greco *et al.*, Phys. Rev. D **84**, 094004 (2011)
[16] K. K. Szabo and A. I. Toth, JHEP **06**, 008 (2003), arXiv:hep-ph/0302255
[17] C. Sasaki and K. Redlich, Phys. Rev. C **79**, 055207 (2009)
[18] R. A. Schneider and W. Weise, Phys. Rev. C **64**, 055201 (2001)
[19] M. A. Thaler, R. A. Schneider, and W. Weise, Phys. Rev. C **69**, 035210 (2004)
[20] A. Peshier, B. Kämpfer, and G. Soff, Phys. Rev. C **61**, 045203 (2000)
[21] B.-J. Schaefer and J. Wambach, Nucl. Phys. A **757**, 479 (2005), arXiv:1604.08454[nucl-th]
[22] H. Ueda, T. Z. Nakano, A. Ohnishi *et al.*, Phys. Rev. D **88**, 074006 (2013)
[23] B.-J. Schaefer, J. M. Pawlowski, and J. Wambach, Phys. Rev. D **76**, 074023 (2007)
[24] K. Kamikado, N. Strodthoff, L. von Smekal *et al.*, Phys. Lett. B **718**, 1044 (2013), arXiv:1207.0400[hep-ph]
[25] R.-A. Tripolt, B.-J. Schaefer, L. von Smekal *et al.*, Phys. Rev. D **97**, 034022 (2018)
[26] N. Tetradis, Nucl. Phys. A **726**, 93 (2003), arXiv:hep-th/0303244
[27] G. Endrődi and G. Markó, JHEP **08**, 036 (2019), arXiv:1905.02103[hep-lat]
[28] M. Wakayama and A. Hosaka, Phys. Lett. B **795**, 548 (2019), arXiv:1905.10956[hep-lat]
[29] Y. Lu, Y.-L. Du, Z.-F. Cui *et al.*, Eur. Phys. J. C **75**, 495 (2015), arXiv:1508.00651[hep-ph]
[30] T. G. Khunjua, K. G. Klimenko, and R. N. Zhokhov, J. Phys. Conf. Ser. **1390**, 012015 (2019), arXiv:1812.01392[hep-ph]
[31] L. Yu, H. Liu, and M. Huang, Phys. Rev. D **94**, 014026 (2016)
[32] Z.-f. Cui, C. Shi, W.-m. Sun *et al.*, The European Physical Journal C **74**, 2782 (2014)
[33] X. Wang, M. Wei, Z. Li *et al.*, Phys. Rev. D **99**, 016018 (2019)
[34] F. Gao and J. M. Pawlowski, Phys. Rev. D **102**, 034027 (2020)
[35] C. Shi, Y.-L. Wang, Y. Jiang *et al.*, JHEP **07**, 014 (2014), arXiv:1403.3797[hep-ph]
[36] Y. Jiang, H. Chen, W.-M. Sun *et al.*, JHEP **04**, 014 (2013)
[37] C. S. Fischer, J. Luecker, and C. A. Welzbacher, Phys. Rev. D **90**, 034022 (2014)
[38] C. S. Fischer, J. Luecker, and J. A. Mueller, Phys. Lett. B **702**, 438 (2011), arXiv:1104.1564[hep-ph]
[39] C. S. Fischer, J. Luecker, and C. A. Welzbacher, Nucl. Phys. A **931**, 774 (2014), arXiv:1410.0124[hep-ph]
[40] C. Shi, Y.-L. Du, S.-S. Xu *et al.*, Phys. Rev. D **93**, 036006 (2016)
[41] F. Gao and Y.-x. Liu, Phys. Rev. D **94**, 094030 (2016)
[42] W.-j. Fu, J. M. Pawlowski, and F. Rennecke, Phys. Rev. D **101**, 054032 (2020)

[43] C. Shi, X.-T. He, W.-B. Jia *et al*., JHEP **06**, 122 (2020), arXiv:2004.09918[hep--ph]
[44] F. Gao and J. M. Pawlowski, Phys. Lett. B **820**, 136584 (2021)
[45] C. S. Fischer, J. Luecker, and J. M. Pawlowski, Phys. Rev. D **91**, 014024 (2015)
[46] G. Eichmann, C. S. Fischer, and C. A. Welzbacher, Phys. Rev. D **93**, 034013 (2016)
[47] Y. Jiang, H. Gong, W.-m. Sun *et al*., Phys. Rev. D **85**, 034031 (2012)
[48] Z.-F. Cui, C. Shi, Y.-H. Xia *et al*., Eur. Phys. J. C **73**, 2612 (2013)
[49] L. Chang, Y.-X. Liu, M. S. Bhagwat *et al*., Phys. Rev. C **75**, 015201 (2007)
[50] S. P. Klevansky, Rev. Mod. Phys. **64**, 649 (1992)
[51] P. Zyla *et al*. (Particle Data Group), PTEP **2020**, 083C01 (2020)
[52] F. Burger, V. Lubicz, M. Müller-Preussker *et al*., Phys. Rev. D **87**, 034514 (2013)
[53] H.-S. Zong and W.-M. Sun, Int. J. Mod. Phys. A **23**, 3591 (2008)
[54] S.-S. Xu, Nucl. Phys. B **971**, 115540 (2021), arXiv:2105.00630[nucl-th]
[55] B.-L. Li, Z.-F. Cui, Z.-H. Yu *et al*., Phys. Rev. D **99**, 043001 (2019)
[56] C.-M. Li, S.-Y. Zuo, Y. Yan *et al*., Phys. Rev. D **101**, 063023 (2020)
[57] Z. Miao, J.-L. Jiang, A. Li *et al*., Astrophys. J. Lett. **917**, L22 (2021), arXiv:2107.13997[astro-ph.HE]